ELSEVIER

Nuclear Instruments and Methods in Physics Research B 193 (2002) 603–608

NIM B
Beam Interactions with Materials & Atoms

www.elsevier.com/locate/nimb

Ion-irradiation-induced defects in bundles of carbon nanotubes

E. Salonen *, A.V. Krasheninnikov, K. Nordlund

Accelerator Laboratory, University of Helsinki, P.O. Box 43, FIN-00014 Helsinki, Finland

Abstract

We study the structure and formation yields of atomic-scale defects produced by low-dose Ar ion irradiation in bundles of single-wall carbon nanotubes. For this, we employ empirical potential molecular dynamics and simulate ion impact events over an energy range of 100–1000 eV. We show that the most common defects produced at all energies are vacancies on nanotube walls, which at low temperatures are metastable but long-lived defects. We further calculate the spatial distribution of the defects, which proved to be highly non-uniform. We also show that ion irradiation gives rise to the formations of inter-tube covalent bonds mediated by carbon recoils and nanotube lattice distortions due to dangling bond saturation. The number of inter-tube links, as well as the overall damage, linearly grows with the energy of incident ions. © 2002 Elsevier Science B.V. All rights reserved.

PACS: 81.07.De; 61.80.Jh; 61.46.+w
Keywords: Carbon nanotubes; Ion irradiation; Molecular dynamics

1. Introduction

Due to their genuine one-dimensional structure, carbon nanotubes are well suited for investigating the effect of disorder on electronic properties of low-dimensional systems. The defects in isolated nanotubes or nanotubes bundled up to ropes can be introduced by employing electron [1,2] or ion [3–5] irradiation. Besides investigating conductivity in low-dimensional systems, studies on irradiated bundles of nanotubes also present considerable interest with a view toward understanding the interaction of nanotubes in bundles [4], their irradiation-induced polymerization through inter-tube sp^3 bonding (nanotube functionalization) [6] or even nanotube coalescence under high-dose electron irradiation [7].

The issue of how electron and ion irradiation influence the structural and electronic properties of individual nanotubes has been addressed recently [1,5,8]. It has been found that the irradiation gives rise to formations of vacancies and other defects on the nanotube walls and to the amorphization of the nanotubes at high irradiation doses. The effects of various defects on the conductance of nanotubes have been also studied [9–13].

The impact of low-dose ion irradiation on bundles of nanotubes has been experimentally investigated as well [4] with a particular stress on the inter-tube coupling resistance. The bundles of nanotubes were irradiated with Ar^+ ion beam at an energy of 500 eV with subsequent transport measurements. The standard program SRIM was used

* Corresponding author. Tel.: +358-9-191-50007; fax: +358-9-191-50042.
E-mail address: msalonen@beam.helsinki.fi (E. Salonen).

0168-583X/02/$ - see front matter © 2002 Elsevier Science B.V. All rights reserved.
PII: S0168-583X(02)00861-3

to characterize the spatial distribution of defects. It was found that the defects are produced in the uppermost 8-nm-thick part of the bundle and the defect vs. depth curve has a single maximum near 3 nm.

It should be noted, however, that the applicability of the SRIM code for estimating the radiation damage at such low energies in highly anisotropic covalent systems like the bundles of nanotubes is questionable. [1] At the same time, a thorough understanding of the microscopical mechanism of inter-tube interaction and electronic transport in the bundles of irradiated nanotubes is not possible without reliable characterization of irradiation-induced defects and their spatial distribution.

In this paper, we study the production of defects in the bundles of single-wall nanotubes under Ar ion [2] irradiation. For this, we make use of an empirical-potential molecular dynamics, which, unlike the SRIM code, takes into account the nature of chemical bonds and particular atom arrangements in the nanotubes and their bundles [14]. Our main goal here is to facilitate the interpretation of the experiments on the irradiation of nanotube bundles and to clarify: (i) What are the defects which appear in bundles of nanotubes under low-dose, low-energy irradiation? (ii) What is the spatial distribution of these defects? (iii) Can ion irradiation give rise to the functionalization of nanotubes, i.e. the formation of covalent, non-planar carbon bonds between the nanotubes?

2. Simulation method

Our molecular dynamics simulation method has been described in detail in other publications [5,15,16] and so only a brief description will be given here.

We simulated the irradiation of a bundle of nanotubes by 100, 250, 500, 750 and 1000 eV Ar ions. For every energy, at least 20 independent runs were carried out for achieving a representative statistics. Similar to experiments in [4], we assumed that the irradiation dose is so low that the average distance between ion impact points is larger than the simulation cell size. Hence, every irradiation event was treated independently of the other. The empirical Brenner potential II [17] was used to model the C–C interactions. [3] However, at short inter-atomic distances the Brenner potential was smoothly joined to the Ziegler–Biersack–Littmark (ZBL) universal repulsive potential [18] in order to model energetic collisions realistically. The ZBL potential was also used to model the Ar–C interactions.

We considered a trigonal lattice of (10,10) armchair nanotubes which are the predominant constituents of the bundles synthesized by the electric arc technique using a catalyst [19]. In compliance with experiments [4], the inter-tube distance in our lattice was 1.7 nm. Our simulation cell consisted of four layers of nanotubes in the direction of the ion beam, since practically all the kinetic energy of ions with energies less than 1 keV was found to be lost within the four uppermost nanotube layers. The length of a single tube was 10 nm. Since the total energy of the system is slightly dependent on the mutual orientation of the nanotubes and many configurations with roughly the same energy are possible, the nanotubes were rotated a random angle about the tube axis before the impact simulations.

The lattice was equilibrated using the Berendsen temperature and pressure control methods [20]. The impact point of the ion was chosen randomly in the central part of the simulation cell. In this work, we considered only normal incidence irradiation. During the impact simulations, the atoms at the simulation cell borders were held fixed in order to model real nanotube bundles, which are

[1] The SRIM code treats the irradiated sample as an amorphous structure, with a homogeneous mass density. Only binary collisions between the ion and the sample atoms are taken into consideration.

[2] The classical MD simulations can not take account of the charge state of atoms. Here we use the term ion to denote the incoming Ar atom regardless of its charge state.

[3] We left out the bond conjugation term from the potential because this speeds up the simulations dramatically, yet we know from previous simulations that this term does not have a profound effect on defect production in carbon nanotubes.

at least three orders of magnitude longer than those used in our simulations. The fixing also enabled us to avoid large displacements of the tubes due to the momentum brought in by the ion. Temperature was scaled within a 2 nm region from the simulation cell borders during the first 10 ps of the simulation runs, after which it was very slowly quenched to 0 K in the whole cell. Removing all the kinetic energy from the system facilitated the analysis of the damage produced by the irradiation. The effects of the irradiation were analyzed visually as well as by calculating the changes in the coordination of the carbon atoms and C–C bond angles.

3. Results and discussion

As follows from our simulations, analogously to the case of isolated single-walled nanotubes [5], the most common defects produced under ion irradiation of bundled-up nanotubes are the atomic vacancies and vacancy-related defects, which vacancies can turn into [1,5,15]. Besides this, topological defects such as Stone–Wales [21] defects were observed. At high temperatures and high irradiation doses the vacancies on the walls are mended via dangling bond saturation and by forming non-hexagonal rings [1]. However, under low-temperature, low-dose irradiation the vacancies in nanotube bundles may survive for macroscopically long times similar to those in isolated irradiated nanotubes [5,15]. Some knocked-off carbon atoms ended up as interstitials and gave rise to various defects both inside nanotubes and in the inter-tube regions. The interstitials can also migrate along the inner or outer surface of the nanotubes and hence result in the annealing of defects.

A typical defect configuration which appeared in a nanotube bundle after 500 eV ion impact and the subsequent relaxation of the carbon network is represented in Fig. 1. In this figure, the irradiation-induced vacancies are obscured by the nanotube walls, but a knocked-off carbon atom adsorbed on the wall inside the nanotube is visible.

Besides this, it is clearly seen that the irradiation gave rise to the formations of inter-tube covalent

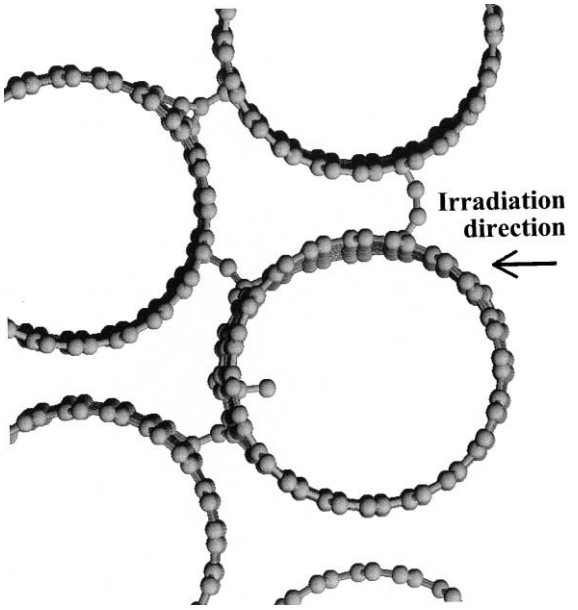

Fig. 1. Ball-and-stick representation (along the tube axes) of the nanotube lattice after a 500-eV Ar impact. Four inter-tube links are clearly visible, as well as a metastable onefold-coordinated atom on the inner wall of the nanotube in the middle of the cell.

bonds mediated by carbon recoils. The saturation of irradiation-induced dangling bonds due to lattice distortion also facilitates the creation of inter-tube links. The majority of these bonds was created between the nanotubes in the adjacent layers (as reckoned from the surface) since in the collisions between the ion and nanotube carbon atoms, the carbon atoms were kicked from their lattice sites downward, deeper into the nanotube matrix. At low energies (100 and 250 eV) the inter-tube coupling took place only in the two topmost layers. The inter-tube bonds also resulted in local distortions of the nanotube carbon network. It should be noted, however, that the inter-tube bonding appears at incident ion energies substantially higher (at least by a factor of two) than the carbon atom knock-on threshold energy (about 50 eV [5]). The irradiation of a nanotube bundle at low energies ($\sim$100 eV) is practically similar to the case of isolated nanotube irradiation.

In order to characterize the spatial distribution of the defects produced by an ion, in Fig. 2 we plot the number of defects as a function of the defect

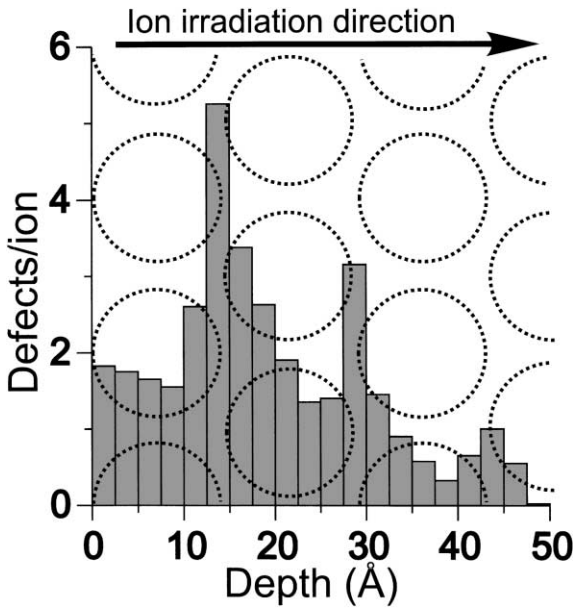

Fig. 2. Number of coordination defects produced per ion (i.e. defect yield) as a function of depth in the 500-eV Ar bombardment simulations. Forty impact simulations were carried out in order to obtain comprehensive statistics. The nanotube lattice is superimposed on the graph in order to visualize the regions where the defects are located. Four peaks are visible in the interface regions between two adjacent layers of nanotubes, where the atomic density is also the largest.

position reckoned from the surface. The values on the ordinate axis correspond to the number of atoms which have a coordination (the number of neighbors) different from three, whereas the values on the abscissa stand for the spatial location of the atoms relative to the surface of the bundle. Thus, if one carbon atom at the very top of the uppermost nanotube is knocked-off from its lattice site, then we will have three (three twofold-coordinated atoms) on the y-axis at zero depth and also a non-zero value near the place where the knocked-off atom is located.

The nanotube lattice is also schematically shown in Fig. 2. It is evident from the diagram that the defect distribution over the depth is non-uniform. The largest numbers of defects were observed in the interface region of two adjacent nanotube layers. This is of no surprise as the atomic density per depth unit is the highest in these regions of the lattice. Primary and secondary collisions in these regions easily give rise to the formation of isolated single vacancies, vacancy clusters and other topological defects which lead to atom coordination numbers different from three. Note that SRIM simulations, which do not take into account the structure of carbon network in the nanotube bundles, give a curve with a single maximum (cf. Fig. 1(b) in [4]). Besides this, the position of the maximum on SRIM-generated curve is at about 3 nm, whereas our simulations gave a value of 1.4 nm, which coincided with the diameter of a (10,10) nanotube. The maximum depth of the defects also differs substantially (5 nm for our molecular dynamics simulations, 8 nm for SRIM). These differences stem likely from ignoring the atomic structure and covalent bonding of the bundled-up nanotubes by SRIM. The number of peaks in the curve is proportional to the energy of incident ions depending on the maximum penetration depth of the ions. At high energies the peaks are broadened due to a larger number of secondary recoils scattered at various angles.

We also stress that, because of the high anisotropy of the nanotube bundles, the spatial distribution of defects is likely to depend on the angle between the nanotube axis and the irradiation direction. However, a detailed study of the effect of the irradiation direction on the defect production is beyond the scope of this study.

The spatial distribution of the defects and the total damage depend strongly on the energy of incident ions as well. The total number of defects (an integral over the depth distributions similar to that shown in Fig. 2) is given in Fig. 3 as a function of the incident ion energy. It is seen that the number of defects grows linearly with the ion energy. This behavior originates from the fact that all ion energy is absorbed in the bundle. A non-linear dependence with a maximum near 600 eV has been reported [5] for isolated nanotubes, since in the latter case at high energies the ion preserves a substantial part of its energy after the penetration through the nanotube.

The number of inter-tube links (see Fig. 4) produced per ion is also directly proportional to the ion energy. The average number of the links increases from 0.75 at 100 eV up to 10.6 at 1000 eV. We stress here once more that our simulations

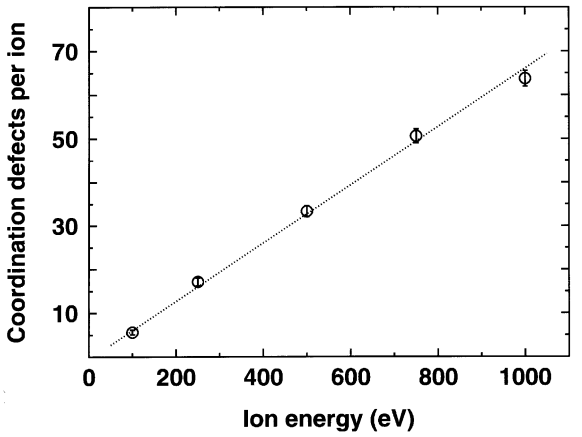

Fig. 3. Number of coordination defects produced per ion impact as a function of energy. The line is a linear fit to the data.

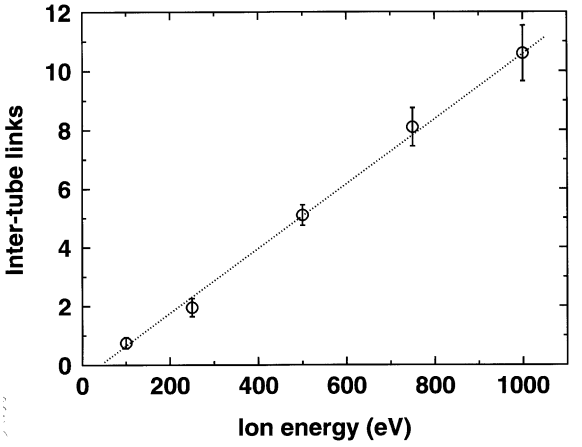

Fig. 4. Number of inter-tube links produced per ion impact as a function of energy. The line is a linear fit to the data.

correspond to the case of low-dose, low-temperature irradiation when the mobility of carbon interstitials and the concentration of ion irradiation-induced defects (and, correspondingly, lattice distortions) are rather low. This topic will be examined elsewhere.

4. Conclusions

In this paper, making use of molecular dynamics, we simulated low-temperature, low-dose 100–1000 eV Ar ion irradiation of bundles of single-wall carbon nanotubes. Our calculations indicate that the most common defects produced at all energies are vacancies on nanotube walls. The vacancies are metastable and can transform to other defect by saturating dangling bonds and deforming the carbon network of nanotubes. The spatial distribution of the defects proved to be highly non-uniform and has several maxima. These maxima are located in the interface regions between nanotubes in different layers, where the atomic density is the highest.

We also demonstrate that ion irradiation gives rise to the formation of inter-tube covalent bonds mediated by carbon recoils and nanotube lattice distortions due to dangling bond saturation. The number of inter-tube links, as well as the overall damage, linearly grows with the energy of incident ions.

Our simulations elucidate the microscopic structure of the irradiation-induced defects in bundles of nanotubes, thus facilitating the interpretation of experiments [4] on the effects of irradiation on inter-tube interaction and electronic properties of nanotube bundles. Our results also indicate that ion irradiation can be employed for the functionalization of nanotubes in bundles, which opens up a new route for modifying mechanical and electronic properties of nanotubes in bundles.

Acknowledgements

The research was supported by the Academy of Finland under projects nos. 44215 and 73722. One of us (E.S.) wishes to thank the Vilho, Yrjö and Kalle Väisälä foundation for travel expense grants. Grants of computer time from the Center for Scientific Computing in Espoo, Finland are gratefully acknowledged.

References

[1] P. Ajayan, V. Ravikumar, J.-C. Charlier, Phys. Rev. Lett. 81 (1998) 1437.
[2] F. Banhart, Rep. Prog. Phys. 62 (1999) 1181.
[3] Y. Zhu, T. Yi, B. Zheng, L. Cao, Appl. Surf. Sci. 137 (1999) 83.
[4] H. Stahl, J. Appenzeller, R. Martel, P. Avouris, B. Lengeler, Phys. Rev. Lett. 85 (2000) 5186.

[5] A.V. Krasheninnikov, K. Nordlund, M. Sirviö, E. Salonen, J. Keinonen, Phys. Rev. B 63 (2001) 245405.
[6] B. Ni, S. Sinnott, Phys. Rev. B 61 (2000) 16343.
[7] M. Terrones, H. Terrones, F. Banhart, J.-C. Charlier, P. Ajayan, Science 288 (2000) 1226.
[8] A.V. Krasheninnikov, Sol. Stat. Comm. 118 (2001) 361.
[9] D. Orlikowski, M.B. Nardelli, J. Bernholc, C. Roland, Phys. Rev. B 61 (2000) 14194.
[10] D. Orlikowski, H. Mehrez, J. Taylor, H. Guo, J. Wang, C. Roland, Phys. Rev. B 63 (2001) 155412.
[11] H.J. Choi, J. Ihm, S. Louie, M. Cohen, Phys. Rev. Lett. 84 (2000) 2917.
[12] A. Hansson, M. Paulsson, S. Stafström, Phys. Rev. B 62 (2000) 7639.
[13] T. Kostyrko, M. Bartkowiak, G.D. Mahan, Phys. Rev. B 60 (1999) 10735.
[14] M.J. López, A. Rubio, J.A. Alonso, L.-C. Qin, S. Iijima, Phys. Rev. Lett. 86 (2001) 3056.
[15] A.V. Krasheninnikov, K. Nordlund, J. Vac. Sci. Technol. B (2002), in press.
[16] K. Nordlund, J. Keinonen, T. Mattila, Phys. Rev. Lett. 77 (1996) 699.
[17] D.W. Brenner, Phys. Rev. B 42 (1990) 9458.
[18] J.F. Ziegler, J.P. Biersack, U. Littmark, The Stopping and Range of Ions in Matter, Pergamon, New York, 1985.
[19] C. Journet, W.K. Maser, P. Bernier, A. Loiseau, M.L. de la Chapelle, S. Lefrant, P. Deniard, R. Lee, J.E. Fischer, Nature 388 (1997) 756.
[20] H.J.C. Berendsen, J.P.M. Postma, W.F. van Gunsteren, A. DiNola, J.R. Haak, J. Chem. Phys. 81 (1984) 3684.
[21] A. Stone, D. Wales, Chem. Phys. Lett. 128 (1986) 501.